# Eddy covariance measurements of carbon exchange and latent and sensible heat fluxes over a boreal lake for a full open-water period

Timo Vesala,[1] Jussi Huotari,[2] Üllar Rannik,[1] Tanja Suni,[3] Sampo Smolander,[1] Andrey Sogachev,[1] Samuli Launiainen,[1] and Anne Ojala[2]

Received 14 June 2005; revised 2 December 2005; accepted 1 February 2006; published 2 June 2006.

[1] Long-term measurements of sensible and latent heat and carbon dioxide fluxes were performed over a boreal lake in southern Finland using the direct micrometeorological eddy covariance (EC) technique. The water column was sampled weekly for dissolved carbon dioxide, and the $CO_2$ flux was estimated also applying the concentration gradient method. Temperature and oxygen profiles of the lake were measured twice a week. The measurements covered one full open-water period from April to November 2003, and it is the longest continuous $CO_2$ record ever measured over a lake by EC. The sensible heat flux $H$ was positive, that is, from the lake to the atmosphere, except in May, when it was >0 W/m$^2$ at night and <0 W/m$^2$ in daytime. The latent heat flux dominated clearly over $H$ in spring and summer; that is, the Bowen ratio was less than 1. Higher-moment turbulence statistics proved to be efficient in detection of frequent nonstationary situations. Applying the statistical criteria for $CO_2$ concentration and vertical wind speed, averaging over a 5-min period and selecting only the wind direction with longest fetch, we could obtain lake-representative $CO_2$ fluxes. Footprint analysis based on a closure model revealed that the source areas were relatively short because of the presence of turbulence generated by the surrounding forest, compared to a larger lake with an extended smooth surface. We observed a net $CO_2$ source of 0.2–0.4 $\mu$mol m$^{-2}$ s$^{-1}$ excluding July, when the flux was closer to zero. The results are consistent with the gradient method, based on more infrequent sampling, and both methods gave the same average flux, 0.2 $\mu$mol m$^{-2}$ s$^{-1}$, over the whole open-water period.

**Citation:** Vesala, T., J. Huotari, Ü. Rannik, T. Suni, S. Smolander, A. Sogachev, S. Launiainen, and A. Ojala (2006), Eddy covariance measurements of carbon exchange and latent and sensible heat fluxes over a boreal lake for a full open-water period, *J. Geophys. Res.*, *111*, D11101, doi:10.1029/2005JD006365.

## 1. Introduction

[2] In the boreal zone, lakes cover approximately 7% of the total land area [*Myneni et al.*, 2001; *Kortelainen et al.*, 2004]. In Finland the average fraction is 10% but can exceed 20% in some parts of the country [*Raatikainen and Kuusisto*, 1990]. Most of the lakes are small and thus in Finland the number of lakes with a surface area less than 0.01 km$^2$ is over 130,000 [*Raatikainen and Kuusisto*, 1990]. In view of the uncertainty in predicting the lake-atmosphere $CO_2$ transfer, comparative measurements on $CO_2$ fluxes are needed to better understand and quantify the environmental controls regulating water-air gas transfer in natural settings [*Donelan et al.*, 2001; *Anderson et al.*, 1999]. Furthermore, recent findings on the role of wetlands, lakes and rivers as conduits of carbon originally fixed by the surrounding terrestrial systems [*Kling et al.*, 1991; *Cole et al.*, 1994; *Richey et al.*, 2002] also emphasize the importance of $CO_2$ exchange to lakes in general. Better knowledge on carbon cycling in lakes and finally the lake-atmosphere $CO_2$ exchange can thus reduce the uncertainties in estimates of terrestrial net ecosystem exchange (NEE) in more northern latitudes [*Ehman et al.*, 2002]: According to *Hanson et al.* [2004], lakes may mineralize and vent to the atmosphere up to 28% of NEE from the surrounding landscape.

[3] In addition to $CO_2$ concentration gradient measurement, the most commonly used technique in $CO_2$ emission measurement over lakes is the closed chamber technique [*Duchemin et al.*, 1999; *Riera et al.*, 1999; *Striegl et al.*, 2001]. Both methods have the advantage of being relatively easy and inexpensive. However, the chambers are prone to some problems like the possible modification of the flow at the water-air interface. The use of chambers also gives rise to the question of the representativeness of the sampling places. The $CO_2$ concentration gradient measurements are often based on temporally sporadic data, and thus integra-

[1]Department of Physical Sciences, University of Helsinki, Helsinki, Finland.
[2]Department of Ecological and Environmental Sciences, University of Helsinki, Lahti, Finland.
[3]CSIRO Marine and Atmospheric Research, Canberra, ACT, Australia.


0148-0227/06/2005JD006365$09.00

tion over time to estimate, for example, annual fluxes can be somewhat problematic [*Sellers et al.*, 1995; *Striegl et al.*, 2001]. As opposed to the chamber technique the micrometeorological measurement technique called eddy covariance (EC) [see, e.g., *Baldocchi*, 2003] does not disturb the water-air interface. Unlike in the other two methods, the fluxes are usually measured continuously, assuming that the methodological requirements, i.e., the presence of steady state turbulent flow, are fulfilled. One of the instrument requirements of the EC flux measurements is a gas analyzer with a fast enough time response to detect turbulent concentration fluctuations.

[4] Since the EC flux measurement can resolve fluxes over periods as short as 30 min and integrates over an area larger than that of chambers, it gives information on the dynamic response of an individual ecosystem to environmental variables [see, e.g., *Edwards et al.*, 1994]. Since a relatively short time (30 min) is required for each single EC data point, major changes in important environmental variables (such as radiation, temperature, wind speed) can usually be at least partly avoided, which improves the detection and analysis of temporal variability, such as diurnal patterns. In the case of small fluxes the data points can be further averaged over longer periods to reveal any longer trends (like intra-annual variability). Then a compromise between minimizing the standard error and retaining a sufficient number of data points is necessary [see, e.g., *Simpson et al.*, 1997]. For $CO_2$, the EC technique has been broadly used for forest ecosystems, whereas for lakes results are scarce. *Anderson et al.* [1999] have used the method for estimating lake-atmosphere $CO_2$ exchange over a small woodland lake in Minnesota, USA, *Morison et al.* [2000] have used it to characterize the productivity of a tropical *Echinochloa* wetland, and *Eugster et al.* [2003] estimated $CO_2$ exchange using also the EC technique on an Arctic Alaskan and midlatitude Swiss lake.

[5] The spatial representativeness of the flux measured with EC is determined by footprint analysis, a tool for locating the source or sink areas upwind from the flux [e.g., *Schmid*, 2002]. The source area size and upwind distance increase with measurement height and with thermal stability. Because of the latter, flux measurements can represent drastically different areas and mixture of ecosystems at night and during daytime. Although simple analytical footprint models such as the one by *Schuepp et al.* [1990] and *Schmid* [1994] have become widely used and integrated into EC software, their validity is restricted, strictly speaking, only to measurements carried out over an extended homogeneous surface with relatively short vegetation cover. The approach based on ensemble-averaged closure models of atmospheric boundary layer flow [*Sogachev and Lloyd*, 2004] allows for simulation of more realistic conditions of flow inhomogeneity, surface heterogeneities and topographical influences [*Sogachev et al.*, 2004]. As a result, the flux contribution and footprint functions depend on the location of the flux measurement point and may significantly deviate from those for a flat terrain. One should pay special attention to this issue when interpreting results from a complex site such as a small lake surrounded by a forest. If the footprint is located entirely above the lake surface, the influence of the land fluxes does not interfere with the EC measurements. However, the measurements can be contaminated also by the effects of the local advection, although the EC method, since it is a method to measure turbulent, not advective fluxes, is robust against such effects [see *Eugster et al.*, 2003]. In the case of lakes, advection from land can be a significant source of $CO_2$ [*Sun et al.*, 1997, 1998].

[6] The main focus of this study is on the turbulent exchange of $CO_2$ between an isolated lake and the atmosphere, but we consider also momentum flux and sensible and latent heat fluxes. On these latter ones a lot of earlier information exists [e.g., *Heikinheimo et al.*, 1999; *Venäläinen et al.*, 1999] that can be used also for validation of the gathered data. For example, under conditions where momentum flux is not directed downward, EC fluxes are not expected to be a direct function of local surface exchange processes [*Eugster et al.*, 2003]. Also, the magnitude of the latent and sensible heat fluxes and their diurnal patterns, especially the location of the daily maximum can be compared with earlier observations. The recording period of this study is one open-water period starting from the end of the spring ice-covered time. Our $CO_2$ flux record is uninterrupted and thus the longest available so far. For instance, *Anderson et al.* [1999] presented data over a 3-year period, but their data are sporadic and consist of 5 separate weeks in spring, summer and fall. The identification of flux dynamics during different seasons is a crucial part of our study. An important part of the study is also modeling of the footprint area size and fluxes in relation to the surrounding environment. Simultaneously with the EC measurements the lake was sampled for water column $CO_2$ concentration in order to get another estimate for $CO_2$ flux; these results were then compared with those obtained with the EC technique.

## 2. Materials and Methods

### 2.1. Site and Measuring Platform

[7] The study lake, Lake Valkea-Kotinen, is situated in the Kotinen nature reserve area in Evo, southern Finland (61°14′N, 25°03′E) (Figure 1). The lake is about 460 m long and 130 m wide with a surface area of 0.041 $km^2$. The maximum and mean depths are 6.5 m and 2.5 m, respectively. The catchment area of the lake, which is 0.30 $km^2$ in size, consists of an old virgin forest and a small area of peatland. Lake Valkea-Kotinen is the uppermost lake of the lake chain and thus it has no inlet, but it does have a small outlet in the shallow southeast end of the lake. The surface inflow through the peatland and peaty forest floor gives the lake its brownish color and the relatively high dissolved organic carbon concentration, i.e., 120 mg Pt $L^{-1}$ Pt (Platinum units) and 11 mg $L^{-1}$, respectively. The water is slightly acidic with an epilimnetic pH of 5.2 and its buffer capacity is very low; that is, alkalinity is approximately 0.003 eq $m^{-3}$. Thus most of the inorganic carbon present in the lake is in the form of $CO_2$. As a brown water lake, Lake Valkea-Kotinen is strongly stratified both thermally and chemically. Stratification starts to build up early in spring, and the lake is thus spring meromictic; that is, the spring turnover is incomplete. In summer the thermocline usually lies at the depth of 2–2.5 m and below that the whole water column is anoxic. Lake Valkea-Kotinen is very productive for a humic lake [*Keskitalo et al.*, 1998]. Because of dark

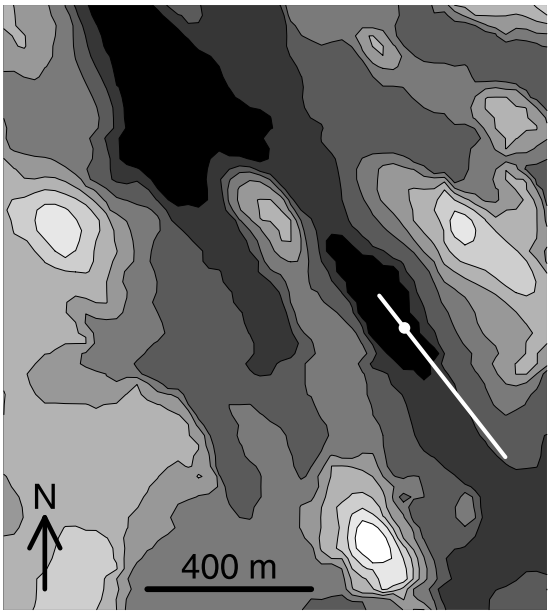


**Figure 1.** Topography map of the area around Lake Valkea-Kotinen. Water bodies are shown in black. Height difference between contour lines is 4 m. The white circle indicates the location of the measurement system, and the white line is the cross section shown in Figure 6.

water color, primary production occurs only within the first 2 m below the surface and during summer $CO_2$ rich hypolimnion is closed off from epilimnion by steep stratification. $CO_2$ is then depleted by primary producers during bright and long days and the possible deficit can only be replaced from the atmosphere. For the monitoring of long-range transboundary air pollution, Lake Valkea-Kotinen with its surrounding catchment area has formed part of the multidisciplinary Integrated Monitoring Programme (ICP IM) since 1990 [*Ruoho-Airola et al.*, 1998].

[8] A platform for the EC equipment was moored approximately 280 m away from the northwest end of the lake and 35 m from the east shore. The platform consisted of three rafts that were attached to each other to form a triangle with each side about 5 m in length. The EC measurement tower was set up on the platform's angle pointing to the longest fetch. When fully loaded, the surface of the platform was 0.35 m above the lake surface.

### 2.2. Eddy Covariance Measurements

[9] The system included a Metek ultrasonic anemometer (USA-1, Metek GmbH, Germany) to measure the three wind speed components and sonic temperature, and a closed-path infrared gas analyzer (LI-7000, Li-Cor, Inc., Lincoln, Nebraska, USA) that measures $CO_2$ and $H_2O$ concentrations. The measurement height was 1.5 m. The length of the stainless steel sampling tube was 1.8 m and the inner diameter was 4 mm. The tube was heated by the power of 3 W/m. Air was filtered by 1 μm PTFE filter and the flow rate was 6.0 L/min providing turbulent flow. The gas analyzer was kept in the temperature-controlled enclosure. Sampling frequency was 20 Hz. The gas analyzer was connected to the anemometer data logger, from which data were recorded by a computer. These trace gas flux instruments are typical of those used in EC flux systems of $CO_2$ and $H_2O$, and their operation has been described extensively in the literature [e.g., *Aubinet et al.*, 2000]. The micrometeorological fluxes of heat, $CO_2$, $H_2O$ and momentum were calculated as covariances between the scalars (temperature or mixing ratio) or horizontal wind speed and vertical wind speed according to commonly accepted procedures [*Aubinet et al.*, 2000]. The 2-D rotation was performed before calculating the fluxes. The flux correction caused by water vapor transfer was performed according to *Webb et al.* [1980]. Heat transfer correction is not required since the temperature fluctuations are damped out in the sampling tube [*Rannik et al.*, 1997].

[10] The flux of $CO_2$ and water vapor is given by [e.g., *Webb et al.*, 1981]

$$F_c = \rho \overline{s'w'} \tag{1}$$

where $s'$ and $w'$ are the instantaneous deviations from the time-averaged values of the mixing ratio and vertical wind component, respectively, and $\rho$ is the density of the dry air. The bar above the product of the fluctuations denotes time averaging. Similarly, the (sensible) heat and kinematic momentum fluxes are

$$H = \rho c_p \overline{T'w'} \tag{2}$$

$$F_m = \overline{u'w'} \tag{3}$$

where $c_p$ is the specific heat of the air at the constant pressure, $T'$ is the temperature fluctuation and $u'$ is the horizontal wind component fluctuation (note that $x$ axis is set parallel to the average horizontal wind direction). Upward fluxes were defined to be positive. For downward (negative) kinematic momentum fluxes the friction velocity is defined by

$$u^* = \sqrt{-F_m} \tag{4}$$

The latent heat flux ($LE$) was obtained by multiplying the water vapor flux by the latent heat of vaporization of water.

[11] The momentum and heat fluxes were averaged over 30-min periods with linear detrending of time series. The final $CO_2$ fluxes were averaged over 5-min periods.

### 2.3. Footprint Analysis

[12] Footprint analysis was performed using the SCADIS model [*Sogachev et al.*, 2004; *Sogachev and Lloyd*, 2004]. SCADIS uses a one-and-a-half-order turbulence closure scheme to simulate turbulent transport in the boundary layer. The model was run in two-dimensional mode for a transect (Figure 1) formed by the main wind directions (Figure 2). For sensitivity tests, we varied the geostrophical wind speed ($v_g$) and surface roughness. For the upper boundary condition, we used $v_g$ of 10 $ms^{-1}$ and 15 $ms^{-1}$ at 3 km height. The mixing length at water surface was varied from 0.1 mm to 10 mm. The old spruce forest on the shore was modeled as 20 m high and having an effective leaf area index (LAI) of 3.8 [*Stenberg et al.*, 1999]. The young spruce forest near the shoreline was 7 m high with

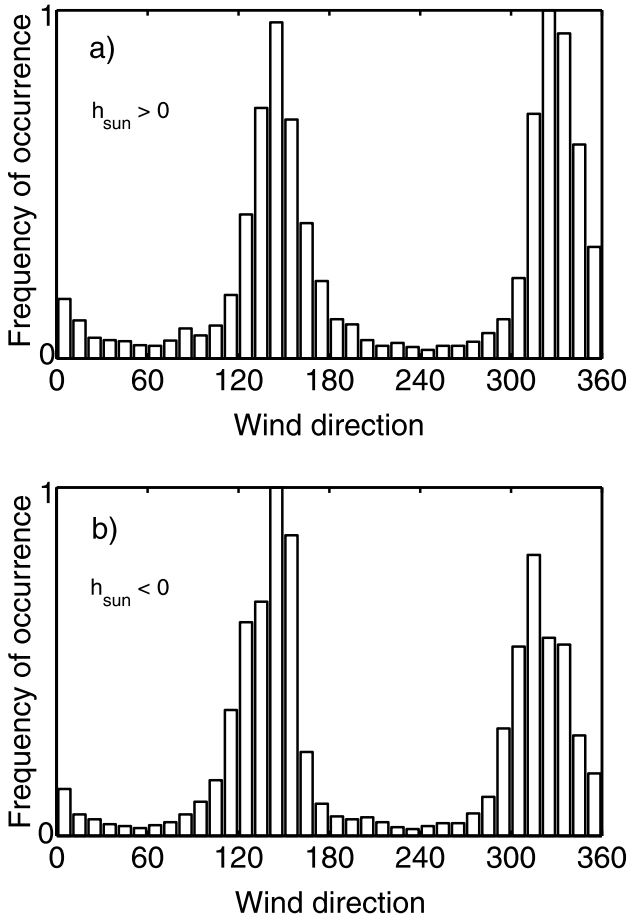


**Figure 2.** Relative frequency distribution of wind direction for (a) day ($h_{sun} > 0$) and (b) night ($h_{sun} < 0$) for May–November 2003. The highest occurrence is normalized to unity.

LAI of 2. In the model, we assumed a neutral stratification since model simulations for stable cases are more inaccurate and the assumption of the neutral stratification provides conservative estimates for unstable cases.

### 2.4. Meteorological and Lake Concentration Gradient Measurements

[13] The mean wind was measured by the anemometer used for EC measurements. The air temperature, relative humidity (RH) and global radiation were observed by a weather station (Davis Instruments Corp., USA).

[14] For calculation of concentration gradients (see below), the water column was sampled for dissolved $CO_2$. The calculations were based on dissolved inorganic carbon concentration (DIC), pH and temperature as described by *Butler* [1982]. The lake was sampled once a week (between 0800 and 1000 local time (LT) (UT + 2)) at the deepest point about 50 m from the platform. For DIC analyses the samples were taken with a tube sampler (2 L Limnos) from the depths of 0, 0.25, 0.5, 1, 2, 3, 4, 5 and 6 m in duplicate 25 mL glass-stoppered bottles so that the bottles were let to overflow at least three times of their own volume to ensure that no air bubbles were left inside. The bottles were taken to laboratory in a darkened icebox and DIC was measured within 3 hours by lowering the pH of the sample with strong acid and measuring the released $CO_2$ with an IR gas analyzer (URAS 3G, Hartmann & Braun AG, Germany). The samples for pH were also taken from the respective depths and measured in the laboratory (Orion Research SA 720 pH/ISE). Temperature and oxygen profiles of the lake were measured twice a week at 0.5 m intervals with an oxygen thermometer (YSI 55, Yellow Springs Instrument Co., Inc., USA).

### 2.5. Concentration Gradient Method

[15] The calculations of fluxes based on concentration gradient of dissolved $CO_2$ followed those of *Cole and Caraco* [1998]:

$$F_g = \alpha k\left(C_{sur} - C_{eq}\right) \tag{5}$$

where $\alpha$ is a chemical enhancement factor that was assumed to be 1 in this slightly acidic soft water lake and $k$ is a piston velocity. C refers to the concentration of $CO_2$ at the surface ($C_{sur}$) and at equilibrium ($C_{eq}$). Note that at equilibrium, when no net flux exists, absolute concentrations in the water and in the air differ from each other by the amount given by Henry's law [see, e.g., *Seinfeld and Pandis*, 1998]. Equilibrium concentration was calculated from truly measured values of atmospheric $CO_2$ concentration. $k$ was normalized to a Schmidt number (Sc) of 600 using the equation [*Crusius and Wanninkhof*, 2003]

$$k_{CO2}/k_{600} = (\mathrm{Sc}_{CO2}/\mathrm{Sc}_{600})^n \tag{6}$$

For $n$ we used $-0.67$ and $\mathrm{Sc}_{CO2}$ was taken from the study by *Jähne et al.* [1987]. $k_{600}$ was calculated using the equation from *Cole and Caraco* [1998]:

$$k_{600} = 2.07 + 0.215U_{10}^{1.7} \tag{7}$$

where $U_{10}$ refers to wind speed at 10 m height. For conversion of our wind speed values to wind speed at 10 m we used the following equation [see *Crusius and Wanninkhof*, 2003]:

$$U_{10} = 1.22U \tag{8}$$

Note that equation (8) does not take into account any stability effects.

### 2.6. Analyzed Periods and Data Selection

[16] Water sampling started on 16 April 2003 and EC measurements on 24 April when the lake was still ice covered. The ice-out date in Lake Valkea-Kotinen was 8 May. The lake froze over on 23 October, but lost its ice cover between 1 and 2 November and stayed open until 21 November. An interrupted freezing pattern is exceptional and has been observed only once before in Lake Valkea-Kotinen during its 15-year monitoring period. Sampling from the water column continued throughout the summer and autumn so that last samples were taken on 19 November just before the second freezeup. EC measurements ended on 10 November. For the analysis the EC data were grouped in monthly periods. For sensible heat, latent heat and momentum flux the integrated periods were May, June–August, September and October–November. For $CO_2$ concentration the periods were May–June, July,

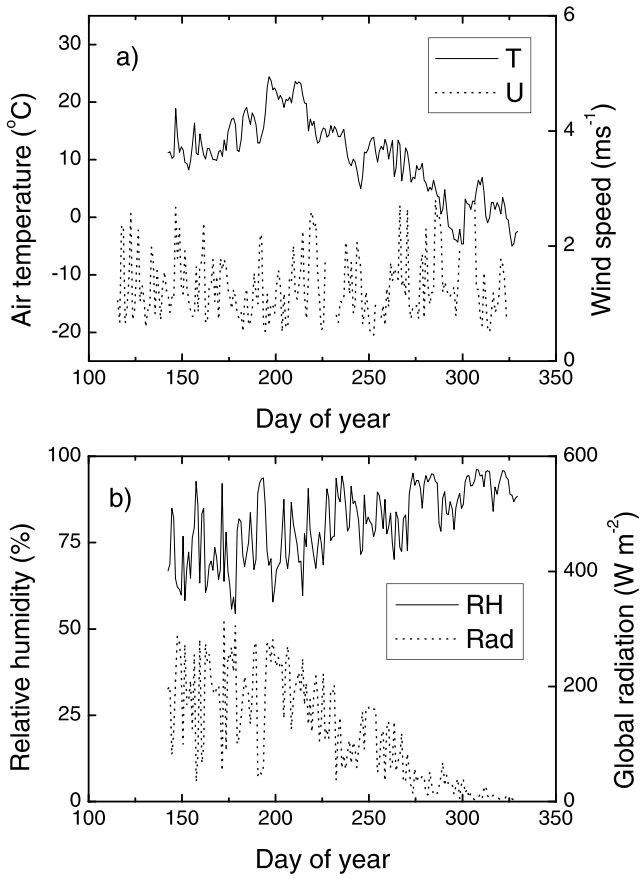


**Figure 3.** Daily (a) air temperature $T$ and wind speed $U$ and (b) relative humidity (RH) and global radiation (Rad) over the open-water period.

August–September and October–November. For $CO_2$ flux we selected monthly periods (October–November was merged since the measurements did not cover the whole November). May and June typically represent the time when the lake is in the state of partial spring turnover after which thermal stratification is growing stronger, July and August represent the month of strongest thermal and chemical stratification, September represents the time when the stratification is breaking up and October–November the time when the fall turnover takes place.

[17] All data when wind is not from the desired direction (110°–170° or 290°–350°, see below) were omitted.

## 3. Results and Discussion

### 3.1. Characterization of Conditions

#### 3.1.1. Meteorological Variables

[18] Figure 3 presents daily averages of air temperature and wind speed (Figure 3a) and RH and global radiation (Figure 3b). The wind speed has typical values and other variables show normal yearly cycles.

[19] According to the frequency distribution of wind direction above the lake for day and night in May–November 2003, the overwhelming majority of flow comes from the directions 110°–170° or 290°–350° (Figure 2). Flow evidently is channeled along the lake, and excluding other wind directions from the data should not greatly affect the measurements. The channeling makes available a large amount of data from the direction of the longest fetch. In all, 33% of the data was omitted because of wind direction (24%) and breaks in measurements (9%).

[20] The monthly grouped diurnal patterns of sensible heat ($H$), latent heat ($LE$) and kinematic momentum flux ($F_m$) are presented in Figure 4. The curves are based on

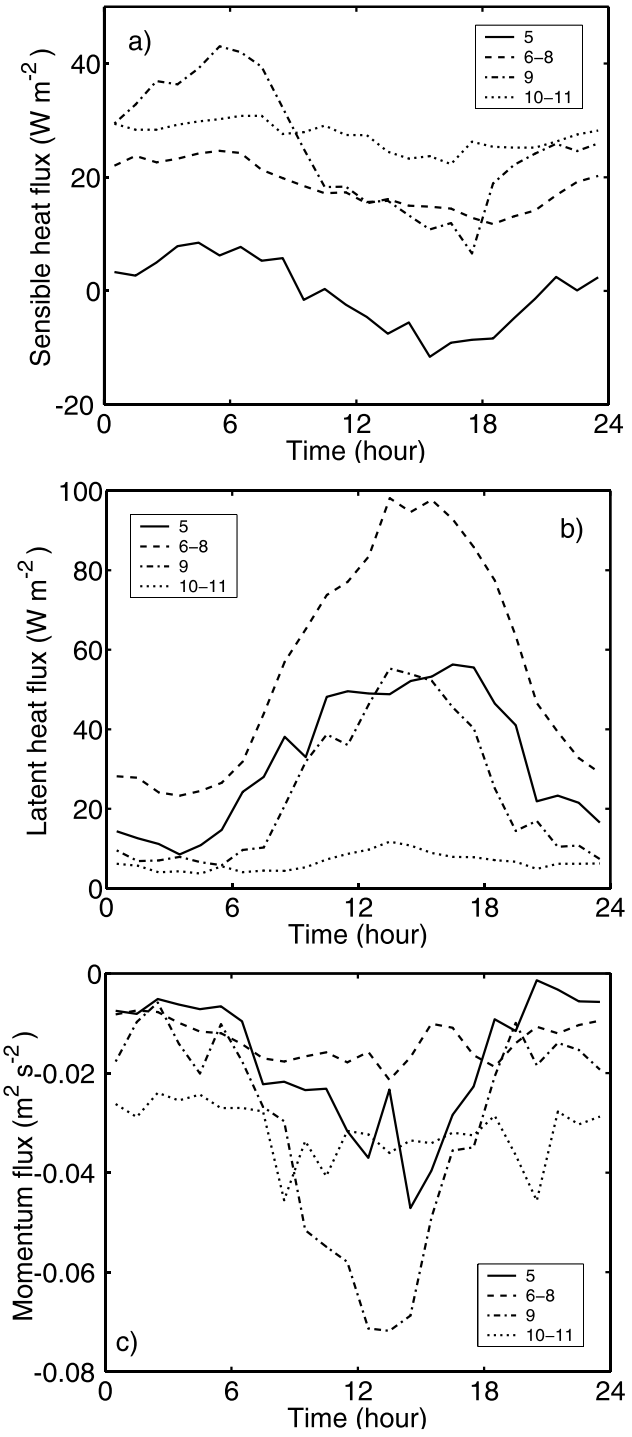


**Figure 4.** Diurnal average curves for (a) sensible heat, (b) latent heat, and (c) kinematic momentum flux for 2003 months (5, May; 6–8, June–August; 9, September; 10–11, October–November) grouped according to similar diurnal pattern.

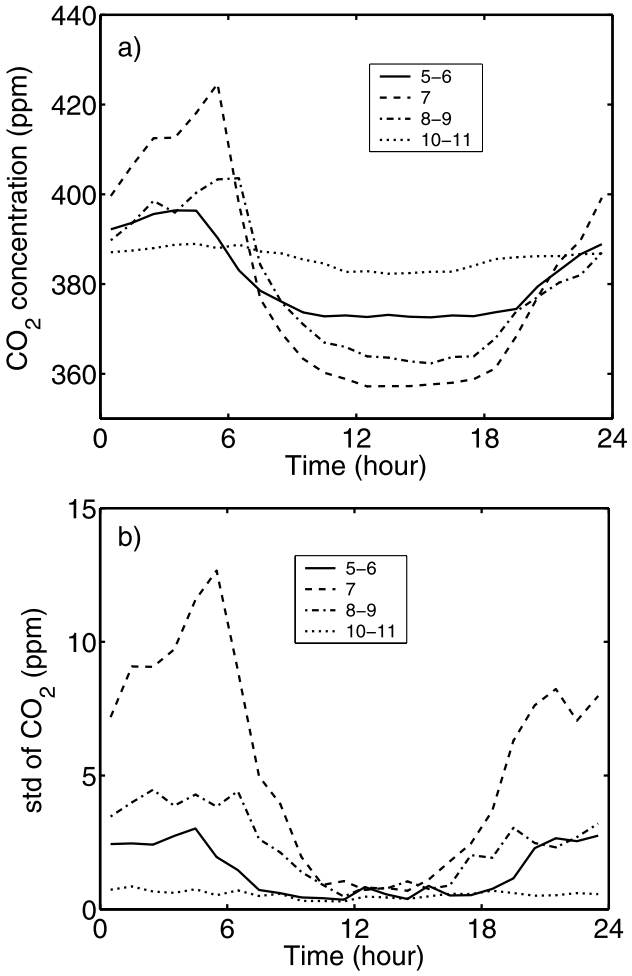


**Figure 5.** Diurnal average curves for (a) $CO_2$ concentration and (b) its standard deviation, for 2003 months (5–6, May–June; 7, July; 8–9, August–September; 10–11, October–November) grouped according to similar diurnal pattern.

hourly averages, and all other wind directions except those along the lake have been excluded. $H$ is always positive, indicating warm air rising upward, except in May, when the diurnal pattern shows that $H$ is clearly above zero at night and below zero in daytime (Figure 4a). In addition to May the diurnal pattern was clear in September whereas in summer and late autumn the diurnal changes were modest. The highest $H$ occurred at night in September.

[21] $LE$ always exhibited a strong diurnal curve except in October–November, and the Bowen ratio ($H/LE$) was smaller than 1 in spring and summer, being above 1 only during September nights and throughout October–November (Figure 4b). This is in sharp contrast with boreal forest ecosystems, where the ratio usually exceeds 1 and creates a deep convective boundary layer in daytime [e.g., *Markkanen et al.*, 2001]. However, the results on $H$ and $LE$ are in accordance with those for other lakes, for example for two boreal Swedish lakes studied by *Heikinheimo et al.* [1999] and *Venäläinen et al.* [1999]. Also the diurnal patterns of $LE$ as well as of $H$ with opposite phases were similar in Lake Valkea-Kotinen and in the Swedish lakes.

[22] The kinematic momentum flux $F_m$ was rather constant and small during June–August (Figure 4c), remaining between $-0.01$ and $-0.02$ $m^2s^{-2}$; this corresponds to friction velocity ($u^*$) ranging from 0.1 to 0.14 $ms^{-1}$. In October–November, $F_m$ was also rather constant but its absolute value clearly higher, ranging from about $-0.025$ to $-0.045$ $m^2s^{-2}$ ($u^*$ from 0.16 to 0.2 $ms^{-1}$). In May and September the diurnal pattern was more pronounced indicating calm nights and relatively windy days, and in September the absolute value of $F_m$ reached a maximum of $-0.07$ $m^2s^{-2}$ ($u^*$ 0.26 $ms^{-1}$). These numbers are still very small compared to values above forest canopies that typically range daily between 0 and $-1.2$ $m^2s^{-2}$ ($u^*$ between 0 and 1 $ms^{-1}$) and are about 0.4 $m^2s^{-2}$ on average ($u^*$ about 0.6 $ms^{-1}$) [e.g., *Suni et al.* 2003a], and they reflect the different surface roughness of the lake and a forest.

### 3.1.2. Air $CO_2$ Concentrations

[23] In summer the diurnal pattern of atmospheric $CO_2$ concentration ($c_{CO2}$) is clear (Figure 5a). Figure 5b shows also the corresponding standard deviation $\sigma_{CO2}$. The diurnal fluctuation of $c_{CO2}$ was most pronounced in July. However,

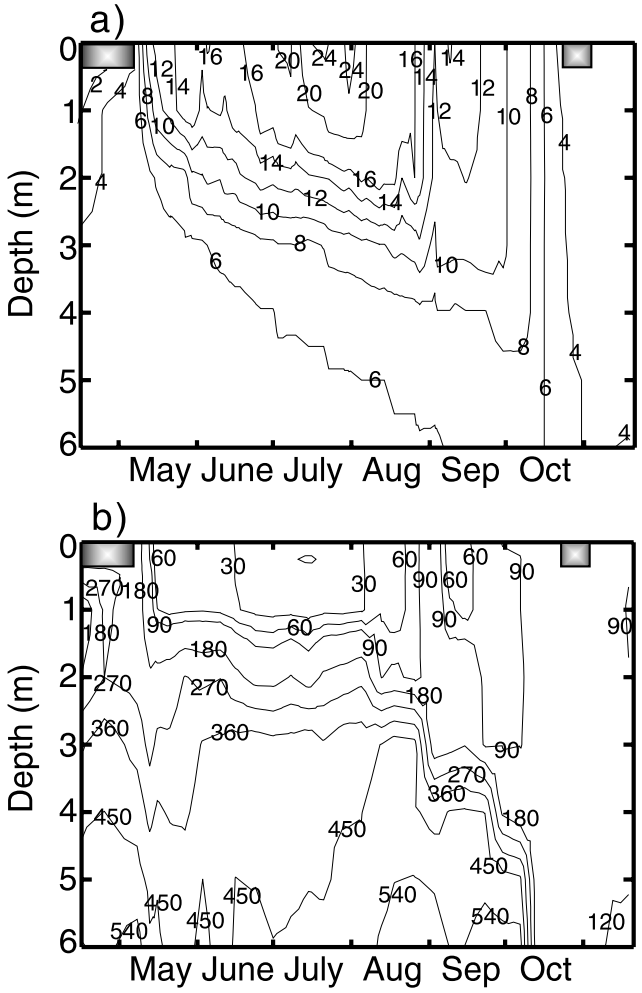


**Figure 6.** (a) Temperature and (b) $CO_2$ concentration (in mmol $m^{-3}$) contours of the lake in 2003. The bars close to surface in April–May and October–November present the ice cover periods.

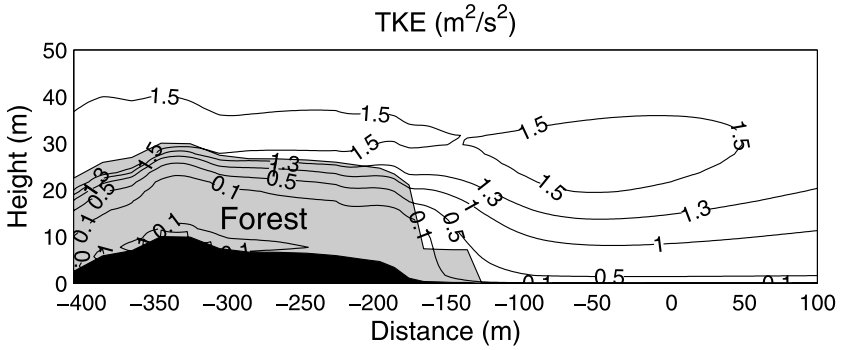


**Figure 7.** Effect of forest edge on the structure of turbulence over the lake, as represented by turbulent kinetic energy (TKE) distribution. Wind direction is from southeast (left) to northwest (right). Geostrophic wind speed was 15 m $s^{-1}$, and the modeled wind speed at the measurement system, located at $x$ = 0 m at 1.5 m height, was 2.2 m $s^{-1}$.

one should note that the footprint of the concentration measurement is large [see, e.g., *Kljun et al.* 2002] and thus $c_{CO2}$ is affected by the surrounding forest. Moreover, during nighttime the flow of $CO_2$ from the forest over the water and subsequent convergence and the vertical transport may be considerable (advection). Simultaneous information on nighttime $\sigma_w$ indicated (not shown) that turbulence was at its smallest, that is mixing was weak. Under such conditions, $CO_2$ released through respiration processes of the lake and forest ecosystem tends to accumulate near the surface.

#### 3.1.3. Lake Variables

[24] In terms of temperature as well as $CO_2$ concentration Lake Valkea-Kotinen was steeply stratified from May till the beginning of October (Figure 6a). In midsummer the surface temperature rose up to 25°C whereas the hypolimnetic temperature was approximately 5°C. When stratified, the thermocline lay at the depth of 1.5 m. Both data sets confirmed the earlier suspicions that the lake is spring meromictic; that is, there is no period of full turn over in May and thus no very large efflux rates are expected. In spring 2003 the mixing depth in Lake Valkea-Kotinen was only approximately 2–2.5 m. In autumn, however, the turn over took place in October at the temperature of 7°C after which the concentration of $CO_2$ stabilized to around 90 mmol $m^{-3}$, i.e., above the equilibrium concentration (Figure 6b). In summer during the stratification period the $CO_2$ concentrations in the epilimnion were always less than 60 mmol $m^{-3}$, and in the surface in midsummer lower than 30 mmol $m^{-3}$ (lowest value 14 mmol $m^{-3}$); at that time the $CO_2$ concentration of the surface water was at or just below the equilibrium. After the incomplete spring turn over the $CO_2$ concentrations in the surface were well above the equilibrium. Below the thermocline the concentration was usually more than 300 mmol $m^{-3}$, i.e., 1 order of magnitude higher than in the surface water. In the anoxic hypolimnion the $CO_2$ concentration increased throughout the stagnation period so that just before the fall turn over the concentrations measured in the very bottom were higher than 500 mmol $m^{-3}$; the maximum was 603 mmol $m^{-3}$ recorded on 26 August.

### 3.2. Footprints

[25] According to the model runs, the most important phenomenon affecting the footprint at the measurement point is the turbulence structure. The turbulence developed over the forest is transported with wind over the lake for several hundred meters (Figure 7). This causes more mechanical turbulence over the lake than would be possible over a wider water body with shores sufficiently far away so that the shoreline vegetation would not have an effect. Further, this increased turbulence causes the footprint of

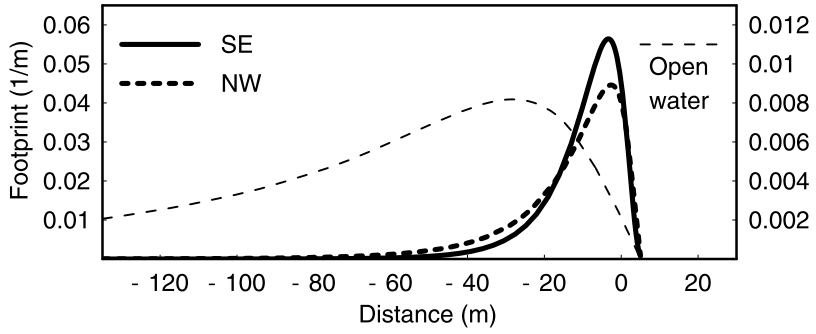


**Figure 8.** Modeled footprints for the two dominant wind directions along the lake: southeast (SE) and northwest (NE). The distance to the forested shore is 135 m in the SE case and 240 m in the NW case (see Figure 1). For comparison, a footprint for a case of open water body without a nearby forested shore is also presented (note 5 times larger scale for the open-water footprint presented on left axis). The measurement height is 1.5 m.

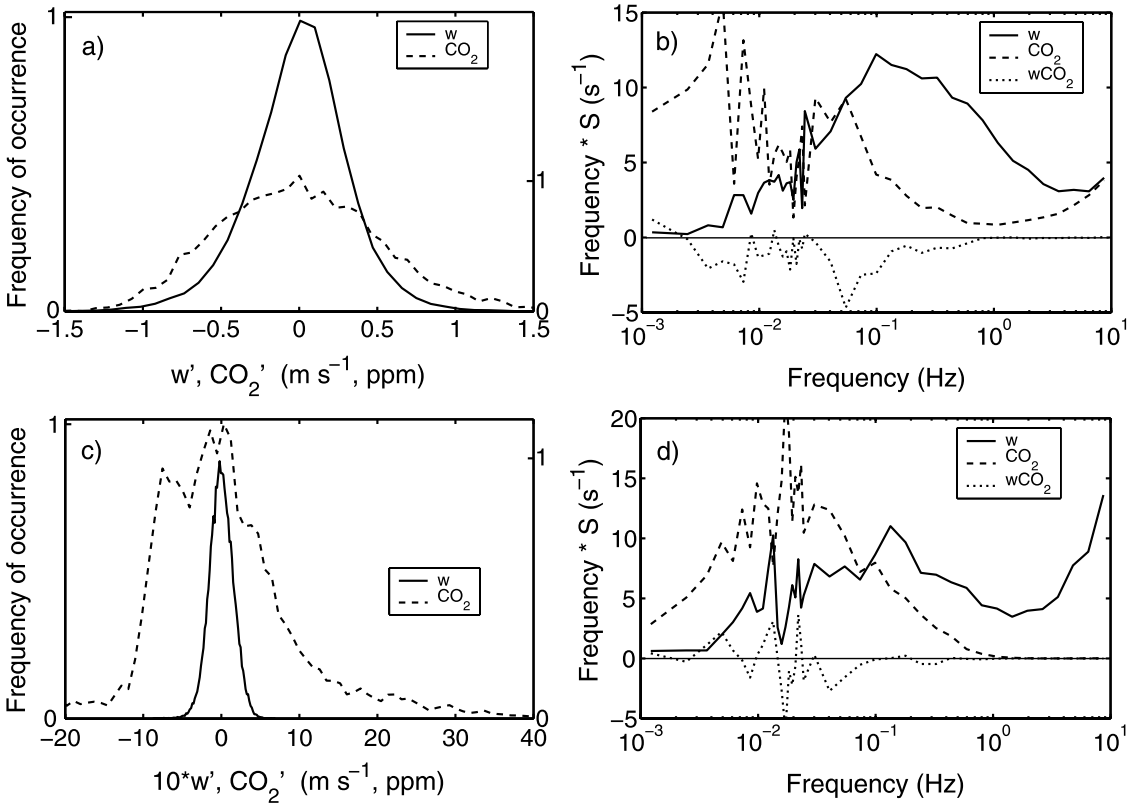


**Figure 9.** Frequency distributions and spectra of turbulent variations measured in (a and b) daytime on 19 June 2003, 1500–1600 LT, and (c and d) nighttime on 19 June 2003, 0400–0500 LT. The highest frequency of occurrence is set at unity. In Figure 9c the wind speed is multiplied by 10. The data do not include the correction caused by water vapor transfer.

the measurements to be smaller compared to a situation over a bigger lake (Figure 8). Also an important factor in the small footprint in the modeled conditions is the low height (1.5 m) of the measurement point. A measurement point higher by only a meter or two would already have footprint reaching the shore in the main wind directions. The footprint results were not sensitive to the values used for water surface mixing length and geostrophic wind speed.

### 3.3. Statistics of Turbulence and $CO_2$ and Water Vapor Fluxes

[26] Next, we consider statistical parameters used in the quality analysis of the measurements. The criteria used for acceptable skewness (*SK*; third statistical moment describing a degree of asymmetry of distribution), kurtosis (*KU*; fourth statistical moment describing a flatness), and flux nonstationarity (*FI*) are less stringent than those proposed for soft flagging by *Mahrt* [1998]. Our criteria were used for identifying behavior that was physical but unusual, often occurring in nonstationary situations. We ended up with the range of −2 to 2, 1 to 8 and <0.3 for acceptable *SK*, *KU* and *FI* values, respectively. For a normal (Gaussian) distribution *SK* is zero and *KU* is 3. Nonstationarity according to a definition by *Foken and Wichura* [1996] corresponds to values >0.3. Prior to calculating *SK* and *KU* statistics, the time series were linearly detrended. In *FI* calculation the time interval used for a calculation of a single flux value is divided into shorter intervals (5-min subrecords) [*Foken and Wichura*, 1996]. If there is a difference of less than 30% between the mean covariances of subrecords and the covariance of the full period, the measurement is considered stationary.

[27] Figure 9 represents frequency distributions, spectra, and cospectra of $c'_{CO2}$ and $w'$ for an example day, 19 July, for both daytime (1500–1600 LT) and nighttime (0400–

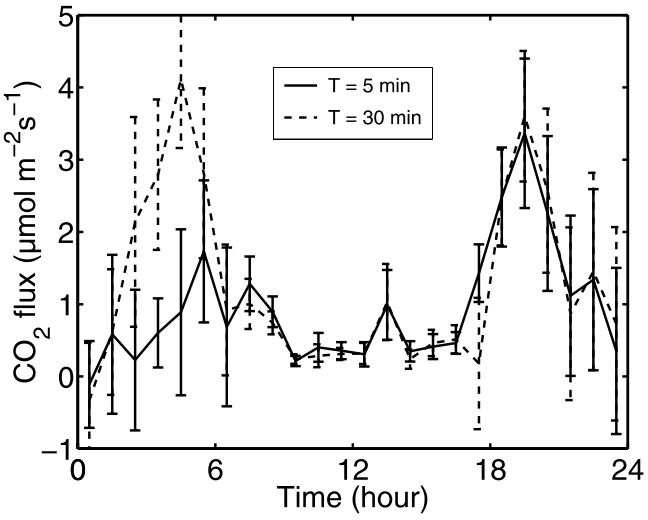


**Figure 10.** Diurnal average curves of $CO_2$ fluxes for July 2003, obtained with 30 min averaging (time series additionally detrended) and 5 min averaging.

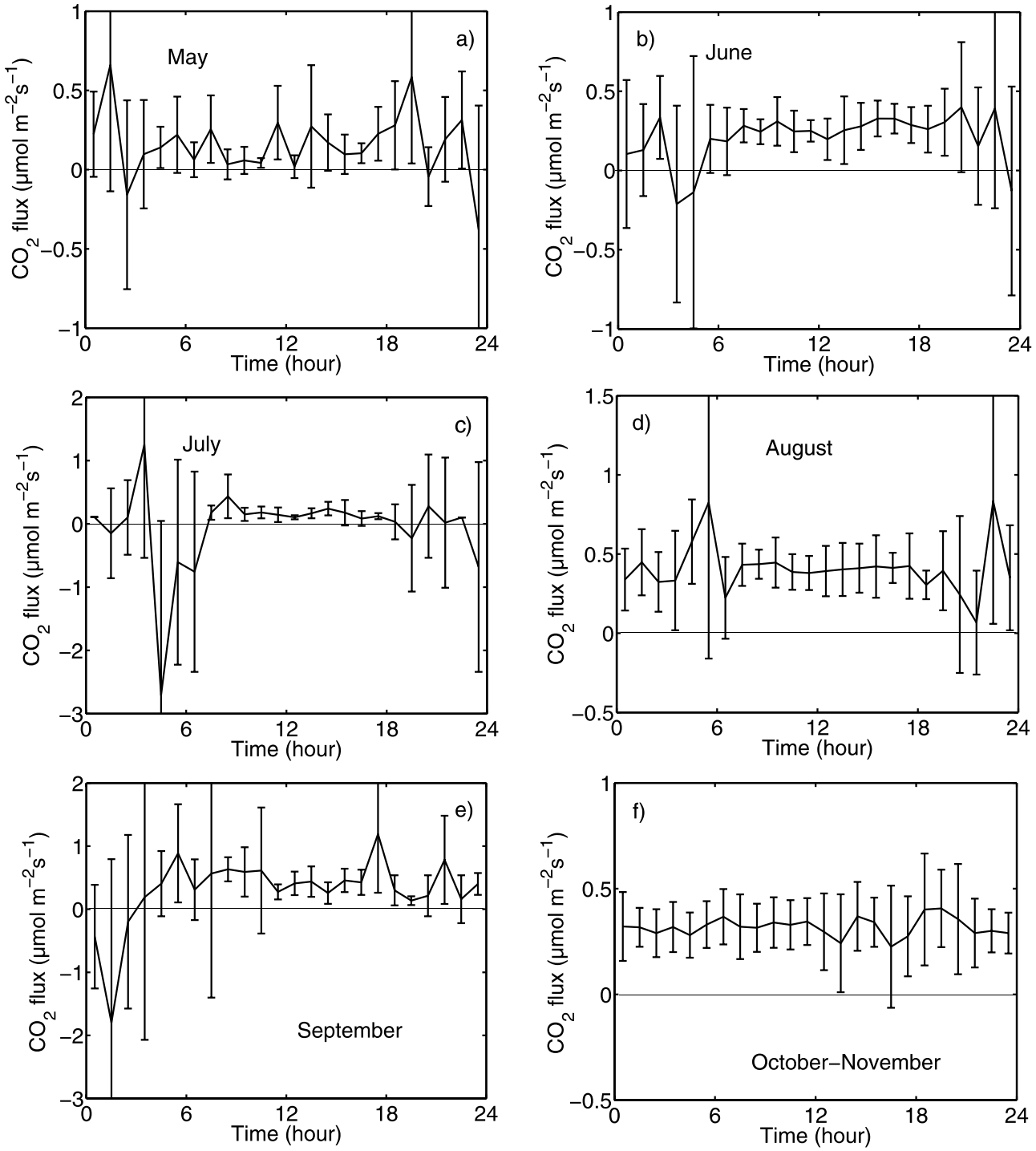


**Figure 11.** Monthly diurnal average $CO_2$ exchange in 2003: (a) May, (b) June, (c) July, (d) August, (e) September, and (f) October–November. The bars present twice the standard error for each hourly average (95% confidence intervals).

0500 LT) (Figures 9a and 9b and Figures 9c and 9d, respectively). The frequency distributions in daytime appear normal, ranging only from about −1.5 to +1.5 ppm for $c'_{CO2}$ and from −1.5 to +1.5 $ms^{-1}$ for $w'$ (Figure 9a). For this period, *SK*, *KU* and *FI* for the data were $SK_w = -0.1$, $SK_{CO2} = 0.3$, $KU_w = 4.7$, $KU_{CO2} = 3.0$, and $FI = 0.04$ (not shown), that is, well within an acceptable range. The spectrum of $w'$ has the accepted shape (Figure 9b), but the spectrum of $c'_{CO2}$ shows a rather large contribution at low frequencies. However, the cospectrum of $w'$ and $c'_{CO2}$ indicates that the measured eddy covariance flux is only weakly affected by the considerable high-frequency noise of individual measurements and the low-frequency variations (Figure 9b).

[28] In comparison to the daytime results, the nighttime data appear somewhat worse (Figures 9c and 9d). The frequency distribution of $w'$ is very similar to that in the

daytime (note that in the figure $w'$ values are multiplied by a factor of 10 for scaling), but the variation of $c'_{CO2}$ is large, ranging over 60 ppm. The cospectrum of $w'$ and $c'_{CO2}$ also shows anomalous features since it varies between positive and negative (Figure 9d). For this period, $SK_w$ = 0.1, $SK_{CO2}$ = 1.0, $KU_w$ = 3.5, $KU_{CO2}$ = 6.9, and $FI$ = 0.31. Although being considerably worse than during daytime these values are still within the acceptable range. Note, however, that during the following three hours $SK_{CO2}$ increased to 4 and $KU_{CO2}$ up to 24 (not shown).

[29] The calculated fluxes were affected by different averaging times, as shown with two different averaging periods, 5 min and 30 min for diurnal average curves of $CO_2$ flux (the time series were additionally detrended) for July (with wind direction only along the lake) (Figure 10). Both averaging periods produced similar behavior in daytime and in the evening, indicating a small source of about 0.5 to 1.0 μmol $m^{-2}s^{-1}$ in daytime and relatively high efflux rates up to about 4 μmol $m^{-2}s^{-1}$ in the evening between 1800 and 2100 LT. However, there is a clear difference between the curves in the morning hours before sunrise: The 30-min averaging produces another peak of high respiration similar to that in the evening, but the 5-min averaging does not. Apparently, filtering (or spectral cutoff of frequencies) affects the flux values so that the longer averaging time takes into account larger eddies than the shorter one, being more prone to the contamination of flux estimates by the surrounding forest.

[30] In all, 77% of the data was omitted because of unsatisfied quality criteria (6%) and wind direction (62%) and breaks in measurements (9%). The fraction of the rejected data is high, but it is normal that 20–30% and 50–60% of eddy covariance day and nighttime data, respectively, is rejected [e.g., *Suni et al.*, 2003b] and further gap filled for nonideal forest sites. Here the site is even more nonideal. Even so the eddy covariance measurements provide more frequent sampling than the traditional concentration gradient method. No gap filling was attempted.

### 3.4. Carbon Exchange

[31] Figure 11 presents the daily courses of monthly $CO_2$ fluxes. As daily sums, the presented plots correspond to values given in Table 1. We also calculated the random uncertainty for the daily sums presuming that for each hourly data point the uncertainty was equal to the error bars given in Figure 11. The lake acted as a source of carbon with an efflux rate varying from 0.2 μmol $m^{-2}$ $s^{-1}$ (May–June) to 0.4 μmol $m^{-2}$ $s^{-1}$ (August). In July the flux was very small. This study was the first long-term $CO_2$ flux measuring campaign on a lake with the EC technique. There are only two published short-term studies with EC on a lake available for comparison. [*Andersson et al.*, 1999] obtained decreasing $CO_2$ fluxes from 2.7 μmol $m^{-2}s^{-1}$ to slightly negative values during a couple of days right after ice melt. Over Toolik Lake in Alaska, *Eugster et al.* [2003] measured summertime fluxes of approximately −0.005 to 0.015 mg C $m^{-2}s^{-1}$ which equal about −0.42 to 1.25 μmol $m^{-2}s^{-1}$, and are thus comparable to our flux values. However, they considered the possibility that downward fluxes did not reach the lake surface because of stable atmospheric conditions.

[32] Finally, we compare the $CO_2$ flux estimates obtained by the concentration gradient and EC methods. It is notable here that the gradient flux calculations are based on water samples that were taken once a week during morning hours and thus their temporal resolution is much worse and the direct comparison of daily and monthly averages is somewhat misleading. However, we provide the comparison since the gradient estimates with infrequent sampling are commonly used for estimates of long-term averages.

**Table 1.** Average Daily Sums of $CO_2$ Exchange Above the Lake in 2003 by Eddy Covariance and the Gradient Method and Random Uncertainties as Estimated From Diurnal Averaging[a]

| Period | Average Daily Sum by EC, μmol $m^{-2}$ $s^{-1}$ | Random Uncertainty (EC), μmol $m^{-2}$ $s^{-1}$ | Average Daily Sum by G, μmol $m^{-2}$ $s^{-1}$ | Random Uncertainty (G), μmol $m^{-2}$ $s^{-1}$ |
|---|---|---|---|---|
| May | 0.16 | 0.12 | 0.31 | 0.28 |
| June | 0.21 | 0.12 | 0.12 | 0.10 |
| July | −0.04 | 0.30 | 0.04 | 0.02 |
| Aug. | 0.39 | 0.12 | 0.23 | 0.12 |
| Sept. | 0.30 | 0.28 | 0.30 | 0.12 |
| Oct.–Nov. | 0.31 | 0.08 | 0.29 | 0.04 |
| May–Nov. | 0.22 | – | 0.22 | – |

[a]See Figure 11. Negative values of average daily sums correspond to uptake of carbon. EC, eddy covariance; G, gradient method. The results are based on data that are not gap filled.

[33] Excluding July, the concentration gradient measurements gave $CO_2$ flux estimates varying from 0.1 μmol $m^{-2}$ $s^{-1}$ (June) to 0.3 μmol $m^{-2}$ $s^{-1}$ (May, September–November) (Table 1), which are generally close to those obtained by EC. Furthermore, the flux decreased strongly in July being 0.04 μmol$m^{-2}s^{-1}$. Thus the general intra-annual variation matches with the EC observations indicating the reduced sink in July. July was also the only month with an observation of undersaturated concentration values indicating an occasional sink. Note that the random uncertainty in the EC results in July is very large. Humic lakes have been considered as a source of atmospheric $CO_2$ throughout the year [e.g., *Riera et al.*, 1999; *Jonsson et al.*, 2003]. Summer 2003 was exceptionally dry and sunny. As a consequence, the water color decreased below 120 mg Pt $L^{-1}$. Thus improved light conditions in the surface layer supported high primary production possibly causing the reduced source of the lake. *Eugster et al.* [2003] found a discrepancy by a factor of 2 between the two methods. Similar discrepancy exists for May–June and August whereas during the autumn months the two methods provide almost identical results. The discrepancy between the results by the two approaches might be reduced by taking gradient samples many times a day. *Sellers et al.* [1995] have also pointed out this issue, and it applies especially to periods when aquatic $CO_2$ exhibits diurnal fluctuation. Nevertheless, both methods gave the same average flux, 0.22 μmol $m^{-2}$ $s^{-1}$, over the whole open-water period.

## 4. Conclusions

[34] The lake in our study was small and oblong, and the wind direction was frequently along the lake, in both directions. This indicates the influence of the lake on local flow patterns (channeling of flow). The sensible and latent heat fluxes were in agreement with earlier studies. The record for $CO_2$ fluxes by the eddy covariance technique is

now the longest available. Applying the statistical criteria for $CO_2$ concentration ($c_{CO2}$) and vertical wind velocity, averaging over a 5-min period and selecting only the wind direction with the longest fetch, we could obtain $CO_2$ fluxes more representative of the lake $CO_2$ exchange. The hourly based eddy covariance measurements were able to reveal reduced source of $CO_2$ in July, otherwise the lake acted as a clear source of $CO_2$. Prior to statistical analysis and data selection, the $CO_2$ fluxes were more affected by larger eddies and showed variable, nonstationary behavior. In the future, longer records on fluxes will be available and this renders possible the analysis of the interannual variability and its connection to biological and climatic forcings.

[35] **Acknowledgments.** This study was supported by Academy of Finland (BORWET, project 201623 and Centre of Excellence "Physics, Chemistry and Biology of Atmospheric Composition and Climate Change"), EU project Carboeurope, Nordic Centre of Excellence NECC, and project REBECCA by Helsinki University Environmental Research Centre (HERC). Lammi Biological Station of University of Helsinki is acknowledged by providing research facilities.

## References

Anderson, D. E., R. G. Striegl, D. I. Stannard, C. M. Micherhuizen, T. A. McConnaughey, and J. W. LaBaugh (1999), Estimating lake-atmosphere $CO_2$ exchange, *Limnol. Oceanogr.*, *44*, 988–1001.

Aubinet, M., et al. (2000), Estimates of the annual net carbon and water exchange of European forests: The EUROFLUX methodology, *Adv. Ecol. Res.*, *30*, 113–175.

Baldocchi, D. D. (2003), Assessing the eddy covariance technique for evaluating carbon dioxide exchange rates of ecosystems: Past, present and future, *Global Change Biol.*, *9*, 479–492.

Butler, J. N. (1982), *Carbon Dioxide Equilibria and Their Applications*, Addison-Wesley, Boston, Mass.

Cole, J., and N. Caraco (1998), Atmospheric exchange of carbon dioxide in a low-wind oligotrophic lake measured by the addition of $SF_6$, *Limnol. Oceanogr.*, *43*, 647–656.

Cole, J. J., N. F. Caracao, G. W. Kling, and T. K. Kratz (1994), Carbon dioxide supersaturation in the surface waters of lakes, *Science*, *265*, 1568–1570.

Crusius, J., and R. Wanninkhof (2003), Gas transfer velocities measured at low wind speed over a lake, *Limnol. Oceanogr.*, *48*, 1010–1017.

Donelan, M. A., W. M. Drennan, E. S. Saltzman, and R. Wanninkhof (Eds.) (2001), *Gas Transfer at Water Surfaces*, *Geophys. Monogr. Ser.*, vol. 127, AGU, Washington, D. C.

Duchemin, E., M. Lucotte, and R. Canuel (1999), Comparison of static chamber and thin boundary layer equation methods for measuring greenhouse gas emissions from large water bodies, *Environ. Sci. Technol.*, *33*, 350–357.

Edwards, G. C., H. H. Neumann, G. den Hartog, G. W. Thurtell, and G. E. Kidd (1994), Eddy correlation measurements of methane fluxes using a tunable diode laser at the Kinosheo Lake tower site during the Northern Wetlands study (NOWES), *J. Geophys. Res.*, *99*, 1511–1517.

Ehman, J. L., H. P. Schmid, C. S. B. Grimmond, J. C. Randolph, P. J. Hanson, C. A. Wayson, and F. D. Cropley (2002), An initial intercomparison of micrometeorological and ecological inventory estimates of carbon exchange in a mid-latitute deciduous forest, *Global Change Biol.*, *8*, 575–589.

Eugster, W., G. Kling, T. Jonas, J. P. McFadden, A. Wüest, S. MacIntyre, and F. S. Chapin III (2003), $CO_2$ exchange between air and water in an Arctic Alaskan and midlatitude Swiss lake: Importance of convective mixing, *J. Geophys. Res.*, *108*(D12), 4362, doi:10.1029/2002JD002653.

Foken, T. H., and B. Wichura (1996), Tools for quality assessment of surface-based flux measurements, *Agric. For. Meteorol.*, *78*, 83–105.

Hanson, P. C., A. I. Pollard, D. L. Bade, K. Predick, S. R. Carpenter, and J. A. Foley (2004), A model of carbon evasion and sedimentation in temperate lakes, *Global Change Biol.*, *10*, 1285–1298.

Heikinheimo, M., M. Kangas, L. Tourula, A. Venäläinen, and S. Tattari (1999), Momentum and heat fluxes over lakes Tämnaren and Råksjö determined by the bulk-aerodynamic and eddy-correlation method, *Agric. For. Meteorol.*, *98–99*, 521–534.

Jähne, B., K. O. Münnich, R. Bösinger, A. Dutzi, W. Huber, and P. Libner (1987), On the parameters influencing air-water gas exchange, *J. Geophys. Res.*, *92*, 1937–1949.

Jonsson, A., J. Karlson, and M. Jansson (2003), Sources of carbon dioxide supersaturation in clearwater and humic lakes in northern Sweden, *Ecosystems*, *6*, 224–235.

Keskitalo, J., K. Salonen, and A.-L. Holopainen (1998), Long-term fluctuations in environmental conditions, plankton and macrophytes in a humic lake, Valkea-Kotinen, *Boreal Environ. Res.*, *3*, 251–262.

Kling, G. W., G. W. Klipphut, and M. C. Miller (1991), Arctic lakes and streams as gas conduits to the atmosphere: Implications for tundra carbon budgets, *Science*, *251*, 298–301.

Kljun, N., M. W. Rotach, and H. P. Schmid (2002), A three-dimensional backward Lagrangian footprint model for a wide range of boundary-layer stratifications, *Boundary Layer Meteorol.*, *103*, 205–226.

Kortelainen, P., H. Pajunen, M. Rantakari, and M. Saarnisto (2004), A large carbon pool and small sink in boreal Holocene lake sediments, *Global Change Biol.*, *10*, 1648–1653, doi:10.1111/j.1365-2486.2004.00848.x.

Mahrt, L. (1998), Flux sampling errors for aircraft and towers, *J. Atmos. Oceanic Technol.*, *15*, 416–429.

Markkanen, T., Ü. Rannik, P. Keronen, T. Suni, and T. Vesala (2001), Eddy covariance fluxes over a boreal Scots pine forest, *Boreal Environ. Res.*, *6*, 65–78.

Morison, J. I. L., M. T. F. Piedade, E. Müller, S. P. Long, W. J. Junk, and M. B. Jones (2000), Very high productivity of the $C_4$ aquatic grass *Echinochloa polystachya* on the Amazon floodplain confirmed by net ecosystem $CO_2$ flux measurements, *Oecologia*, *125*, 400–411.

Myneni, R. B., J. Dong, C. J. Tucker, R. K. Kauffman, P. E. Kauppi, J. Liski, L. Zhou, V. Alekseyev, and M. K. Hughes (2001), A large carbon sink in the woody biomass of northern forests, *Proc. Natl. Acad. Sci. U. S. A.*, *98*, 14,784–14,789.

Raatikainen, M., and E. Kuusisto (1990), Suomen järvien lukumäärä ja pinta-ala, *Terra*, *102*, 97–110.

Rannik, Ü., T. Vesala, and R. Keskinen (1997), On the damping of temperature fluctuations in a circular tube relevant to the eddy-covariance measurement technique, *J. Geophys. Res.*, *102*, 12,789–12,794.

Richey, J. E., J. M. Melack, A. K. Aufdenkampe, V. M. Ballester, and L. L. Hess (2002), Outgassing from Amazonian rivers and wetlands as a large tropical source of atmospheric $CO_2$, *Nature*, *416*, 617–620.

Riera, J. L., J. E. Schindler, and T. K. Kratz (1999), Seasonal dynamics of carbon dioxide and methane in two clear-water lakes and two bog lakes in northern Wisconsin, U.S.A., *Can. J. Fish. Aquat. Sci.*, *56*, 265–274.

Ruoho-Airola, T., S. Syri, and G. Nordlund (1998), Acid deposition trends at the Finnish Integrated Monitoring catchments in relation to emission reductions, *Boreal Environ. Res.*, *3*, 205–219.

Schmid, H. P. (1994), Source areas for scalar and scalar fluxes, *Boundary Layer Meteorol.*, *67*, 293–318.

Schmid, H. P. (2002), Footprint modeling for vegetation atmosphere exchange studies: A review and perspective, *Agric. For. Meteorol.*, *113*, 159–183.

Schuepp, P. H., M. Y. Leclerc, J. I. MacPherson, and R. L. Desjardins (1990), Footprint prediction of scalar fluxes from analytical solutions of the diffusion equation, *Boundary Layer Meteorol.*, *50*, 355–373.

Seinfeld, J. H., and S. N. Pandis (1998), *Atmospheric Chemistry and Physics: From Air Pollution to Climate Change*, John Wiley, Hoboken, N. J.

Sellers, P., R. H. Hesslein, and C. A. Kelly (1995), Continuous measurements of $CO_2$ for estimation of air-water fluxes in lakes: An in situ technique, *Limnol. Oceanogr.*, *40*, 575–581.

Simpson, I. J., G. C. Edwards, G. W. Thurtell, G. den Hartog, H. H. Neumann, and R. M. Staebler (1997), Micrometeorological measurements of methane and nitrous oxide exchange above a boreal aspen forest, *J. Geophys. Res.*, *102*, 29,331–29,341.

Sogachev, A. Y., and J. J. Lloyd (2004), Using a one-and-a-half order closure model of the atmospheric boundary layer for surface flux footprint estimation, *Boundary Layer Meteorol.*, *112*, 467–502.

Sogachev, A., Ü. Rannik, and T. Vesala (2004), On flux footprints over the complex terrain covered by a heterogeneous forest, *Agric. For. Meteorol.*, *127*, 143–158.

Stenberg, P., T. Kangas, H. Smolander, and S. Linder (1999), Shoot structure, canopy openness, and light interception in Norway spruce, *Plant Cell Environ.*, *22*(9), 1133–1142.

Striegl, R. G., P. Kortelainen, J. P. Chanton, K. P. Wickland, G. C. Bugna, and M. Rantakari (2001), Carbon dioxide partial pressure and $^{13}C$ content of north temperate and boreal lakes at spring ice melt, *Limnol. Oceanogr.*, *46*, 941–945.

Sun, J., D. H. Lenschow, L. Mahrt, T. L. Crawford, K. J. Davis, S. P. Oncley, J. I. MacPherson, Q. Wang, R. J. Dobosy, and R. L. Desjardins (1997), Lake-induced atmospheric circulations during BOREAS, *J. Geophys. Res.*, *102*, 29,155–29,166.

Sun, J., R. Desjardins, L. Mahrt, and I. MacPherson (1998), Transport of carbon dioxide, water vapor, and ozone by turbulence and local circulation, *J. Geophys. Res.*, *103*, 25,873–25,885.

Suni, T., J. Rinne, A. Reissell, N. Altimir, P. Keronen, Ü. Rannik, M. Dal Maso, M. Kulmala, and T. Vesala (2003a), Long-term measurements of surface fluxes above a Scots pine forest in Hyytiälä, southern Finland, 1996–2001, *Boreal Environ. Res.*, *8*, 287–301.

Suni, T., F. Berninger, T. Markkanen, P. Keronen, Ü. Rannik, and T. Vesala (2003b), Interannual variability and timing of growing-season $CO_2$ exchange in a boreal forest, *J. Geophys. Res.*, *108*(D9), 4265, doi:10.1029/2002JD002381.

Venäläinen, A., M. Frech, M. Heikinheimo, and A. Grelle (1999), Comparison of latent and sensible heat fluxes over boreal lakes with concurrent fluxes over a forest: Implications for regional averaging, *Agric. For. Meteorol.*, *98–99*, 535–546.

Webb, E. K., G. I. Pearman, and R. Leuning (1980), Correction of flux measurements for density effects due to heat and water vapour transfer, *Q. J. R. Meteorol. Soc.*, *106*, 85–100.

J. Huotari and A. Ojala, Department of Ecological and Environmental Sciences, University of Helsinki, Niemenkatu 73, FIN-15140 Lahti, Finland.

S. Launiainen, Ü. Rannik, S. Smolander, A. Sogachev, and T. Vesala, Department of Physical Sciences, P. O. Box 64, FIN-00014, University of Helsinki, Finland. (timo.vesala@helsinki.fi)

T. Suni, CSIRO Marine and Atmospheric Research, G. P. O. Box 1666, Canberra, ACT 2601, Australia.